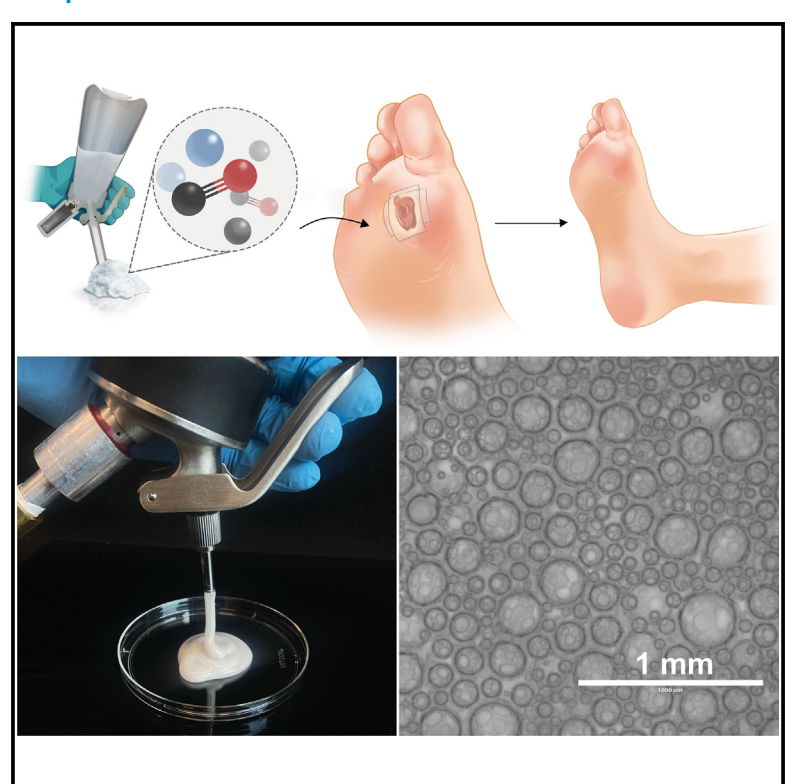
# **Device**

# Modulation of diabetic wound healing using carbon monoxide gas-entrapping materials

# **Graphical abstract**



# **Authors**

Emily Witt, Alexander J. Leach, Jianling Bi, ..., Giovanni Traverso, Leo E. Otterbein, James D. Byrne

# Correspondence

lotterbe@bidmc.harvard.edu (L.E.O.), james-byrne@uiowa.edu (J.D.B.)

#### In brief

Nonhealing diabetic wounds are common in patients with diabetes. Our study utilized FDA-approved gas-entrapping materials for controlled carbon monoxide release. This technique improved dermal fibroblast function, reduced proinflammatory cytokines, and accelerated wound closure in mice, indicating the potential for gas-entrapping materials to enhance diabetic wound healing without drugs.

# **Highlights**

- Topical delivery of CO is feasible using gas-entrapping materials
- Topical delivery of CO resulted in high local and low systemic levels of CO
- CO gas-entrapping materials can improve wound healing in diabetic mouse models





**Device** 



# **Article**

# Modulation of diabetic wound healing using carbon monoxide gas-entrapping materials

Emily Witt, 1,2,3,14 Alexander J. Leach, 3,4,14 Jianling Bi, 1,2,3 Samual Hatfield, 3,4 Alicia T. Cotoia, 5 Megan K. McGovern, 1,2,3,14 Arielle B. Cafi, 1,2,3 Ashley C. Rhodes, 1,2,3 Austin N. Cook, 1,2,3 Slyn Uaroon, 3,6 Bishal Parajuli, 7 Jinhee Kim, 8,9 Vivian Feig, 9,10 Alexandra Scheiflinger, 11 Ikenna Nwosu, 3,4 Miguel Jimenez, 8,5,12 Mitchell C. Coleman, 2,13 Marisa R. Buchakjian, 3,6 Dustin E. Bosch, <sup>3,7</sup> Michael S. Tift, <sup>5</sup> Giovanni Traverso, <sup>9,10,12</sup> Leo E. Otterbein, <sup>11,14,\*</sup> and James D. Byrne<sup>1,2,3,13,14,15,\*</sup>

THE BIGGER PICTURE Wound healing presents a unique challenge for patients with diabetes. Gas therapies have gained significant attention in the wound-healing community. Carbon monoxide (CO) is a small molecule that is well known for its immune-modulating properties when administered at sublethal concentrations. CO is currently in clinical trials for lung disease, sickle cell anemia, and organ transplantation. Here, we investigated the effects of CO in an in vitro wound-healing model and subsequently developed and tested CO gas-entrapping materials (CO-GEMs) for topical application on wounds to promote healing. In this study, we report the efficacy of CO-GEMs in treating full-thickness wounds and pressure ulcers in diabetic mouse models. Collectively, our findings demonstrate that these novel gas entrapping materials could serve as an alternative therapy to both protect the wound bed and promote healing and replace bulky hyperbaric chambers, standard gauze wound dressings, or expensive skin grafts.

#### **SUMMARY**

Diabetic wound healing is uniquely challenging to manage due to chronic inflammation and heightened microbial growth from elevated interstitial glucose. Carbon monoxide (CO), widely acknowledged as a toxic gas, is also known to provide unique therapeutic immune-modulating effects. To facilitate delivery of CO, we have designed hyaluronic-acid-based CO gas-entrapping materials (CO-GEMs) for topical and prolonged gas delivery to the wound bed. We demonstrate that CO-GEMs promote the healing response in murine diabetic wound models (full-thickness wounds and pressure ulcers) compared to N<sub>2</sub>-GEMs and untreated controls.

#### **INTRODUCTION**

In the United States alone, the financial burden from diabetesrelated complications equates to approximately \$237 billion in direct medical costs and a staggering \$90 billion in lost economic productivity. 1 A notorious complication of diabetes is impaired wound healing. This impairment can culminate in chronic skin ulcers for up to 25% of patients with diabetes, leading to increased risk of wound infection, amputation, and even death.2

The foundation of impaired wound healing encompasses various interconnected factors, such as vascular complications,



<sup>&</sup>lt;sup>1</sup>Department of Biomedical Engineering, University of Iowa, Iowa City, IA 52242, USA

<sup>&</sup>lt;sup>2</sup>Department of Radiation Oncology, University of Iowa, Iowa City, IA 52242, USA

<sup>&</sup>lt;sup>3</sup>Holden Comprehensive Cancer Center, University of Iowa, Iowa City, IA 52242, USA

<sup>&</sup>lt;sup>4</sup>Carver College of Medicine, University of Iowa, Iowa City, IA 52242, USA

<sup>&</sup>lt;sup>5</sup>Department of Biology and Marine Biology, University of North Carolina Wilmington, Wilmington, NC 28403, USA

<sup>&</sup>lt;sup>6</sup>Department of Otolaryngology, University of Iowa, Iowa City, IA 52242, USA

<sup>&</sup>lt;sup>7</sup>Department of Pathology, University of Iowa, Iowa City, IA 52242, USA

<sup>&</sup>lt;sup>8</sup>Department of Pharmacology and Toxicology, University of Toronto, Toronto, ON M5S 1A8, Canada

<sup>&</sup>lt;sup>9</sup>Division of Gastroenterology, Brigham and Women's Hospital, Harvard Medical School, Boston, MA 02115, USA

¹ºDavid H. Koch Institute for Integrative Cancer Research, Massachusetts Institute of Technology, Cambridge, MA 02139, USA

<sup>&</sup>lt;sup>11</sup>Department of Surgery, Beth Israel Deaconess Medical Center, Harvard Medical School, Boston, MA 02215, USA

<sup>&</sup>lt;sup>12</sup>Department of Mechanical Engineering, Massachusetts Institute of Technology, Cambridge, MA 02139, USA

<sup>&</sup>lt;sup>13</sup>Free Radical and Radiation Biology Program, University of Iowa, Iowa City, IA 52242, USA

<sup>&</sup>lt;sup>14</sup>These authors contributed equally

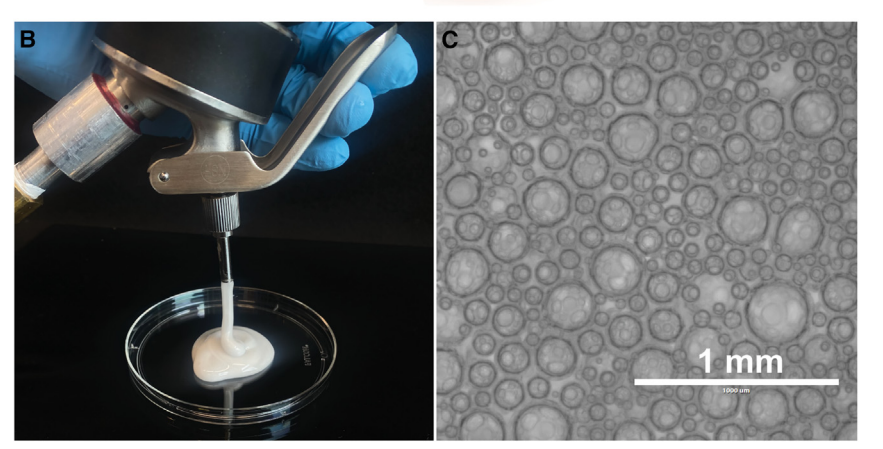
<sup>15</sup>Lead contact

<sup>\*</sup>Correspondence: lotterbe@bidmc.harvard.edu (L.E.O.), james-byrne@uiowa.edu (J.D.B.) https://doi.org/10.1016/j.device.2024.100320









chronic inflammation from altered immune function, and the inflammatory repercussions of persistent hyperglycemia.<sup>3</sup> These conditions impede the functionality of immune cells, disrupt collagen production, and reduce blood flow, making the delivery of crucial oxygen and nutrients to extremities problematic.4 Consequently, processes pivotal for effective wound healing, such as cell proliferation, migration, and tissue remodeling, are compromised.5,6

Traditionally, diabetic wound management has revolved around surgical debridement, topical therapies, and hyperbaric oxygen therapy.<sup>4,7</sup> However, these treatments have shown inconsistent outcomes and present logistical barriers due to access to these therapies.8 Furthermore, the high cost of treating nonhealing wounds in patients with diabetes is a barrier to care for many patients. Pecent studies have highlighted the potential of topical gas therapies in modulating the wound-healing process. 10-13 In fact, gas therapies foster local vasodilation, angiogenesis, and oxidative stress reduction, acting synergistically to promote wound healing and, in turn, reducing bacterial growth. 10,14,15

Here, we introduce molecular gastronomy-inspired, gas-entrapping materials (GEMs) to promote wound healing through engineering strategies to deliver gases, including CO, directly to the wound bed, and these are combined with silver nanoparticles for enhanced wound healing. In our study, we explored the effects of topically applied CO-GEMs on cutaneous wounds (fullthickness wounds and pressure ulcers) in diabetic animal models. This innovative approach seeks to address the challenges posed by traditional treatments and provides a promising avenue for enhancing diabetic wound healing.

#### Figure 1. Application of CO-GEMs for diabetic wound healing

(A) Schematic illustrating how carbon monoxide gas-entrapping materials (CO-GEMs) are administered to diabetic wounds.

(B and C) Pressurized vessel for the creation of CO-GEMs (B) and a microscopic image of a CO-GEM

#### **RESULTS**

# **CO-GEMs** engineered to promote wound healing

To generate and test topical gas delivery systems for wound healing, we created a unique class of GEMs that can be applied to the skin as a cream or ointment. The schematic in Figure 1A shows how GEMs are administered and used for wound healing. The GEMs were created using commercially available whipping siphons to physically entrap gas in materials that are considered generally recognized as safe (GRAS) by the US Food and Drug Administration (FDA). Figure 1A shows how GEMs are administered and can be applied to wounds. These pressurized

whipping vessels were reverse engineered to introduce specific gases within a GEM matrix, as reported previously. 16,17 A custom-made connector facilitates pressurization with any gas. and a one-way valve was incorporated to maintain gas pressure. Figure 1B shows the whipping siphon and macroscopic image, and Figure 1C shows a representative microscopic image of the GEMs that it generates.

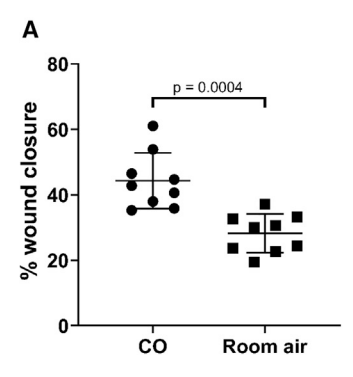
Next, we wanted to test if CO could directly modulate in vitro wound healing as has been reported previously in endothelial cells.<sup>18</sup> To investigate the effect of CO on wound healing, we exposed human dermal fibroblasts to 250 ppm CO or room air and observed enhanced cell migration in cells exposed to CO when compared to room-air-treated cells (Figures 2A and 2B). There was no difference in cell viability of human dermal fibroblasts after daily CO exposure for 8 days (Figure S1). Cells reached confluency by 8 days.

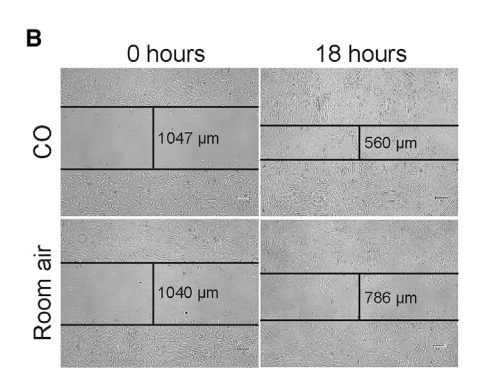
# Hyaluronic-acid-based GEMs physically entrap large quantities of gas and exhibit shear-thinning properties

To further promote wound healing and entrap various gases for testing, we created GEMs using high-molecular-weight hyaluronic acid and silver nanoparticles. Hyaluronic acid is used in a variety of skin substitutes for wound healing. 19 Moreover, silver nanoparticles have been shown to promote wound healing as a result of their antimicrobial properties.<sup>20</sup> Prior to GEM formation, we tested cell viability of human dermal fibroblasts with increasing concentrations of pre-foam solution and found no cytotoxicity up to 4 mg/mL (Figure S2). We then generated two different GEMs-one containing CO and the other containing nitrogen  $(N_2)$ . Due to the inert and similarly anoxic nature of  $N_2$  compared









to CO, N<sub>2</sub> was used as the control for subsequent wound-healing experiments. The concentration of each gas in the GEM was found to be 1 mg/g (Figure 3A), which is consistent with our prior studies. $^{16,17}$  The concentration of CO in the GEM is  $\sim$ 44 times higher than prior work using polyacrylic acid systems (Figure S3). 14 The CO- and N<sub>2</sub>-GEMs formulated with 1.0 weight % (wt %) hyaluronic acid had similar gas release kinetics, with the gas fully released by 24 h (Figures 3B and S4). Moreover, we found that the stability of GEMs was directly correlated with the hyaluronic acid concentration (Figure 3C).

Next, we assessed the performance of the GEMs under flow conditions. The GEMs exhibited behavior akin to viscoelastic solids, with the storage moduli (G") showing an increase corresponding to the concentration of hyaluronic acid, surpassing the loss moduli (G") across all formulations (Figure 3D). Further, all formulations demonstrated high shear-thinning characteristics, indicating their suitability for facile deployment through spraying or injection (Figure 3D). Notably, the GEM comprising 1.0 wt % hyaluronic acid displayed the ability to quickly transition between flow-like and solid-like behavior at high and low shear strains, respectively (Figure 3E). Consequently, the formulation with 1.0 wt % hyaluronic acid was selected as the lead CO-GEM for further evaluation in small-animal models.

Next, we wanted to test if our lead CO-GEM could directly modulate in vitro wound healing similar to CO gas. To investigate the effect of CO on wound healing, we exposed human dermal fibroblasts to the CO-GEM or the room air-GEM and observed enhanced cell migration in cells exposed to the CO-GEM when compared to room air-treated cells (Figure S5).

# Topical application of CO-GEMs resulted in high local and low systemic levels of CO

An important goal of any CO-based therapy is to maintain safe levels of CO exposure while maximizing therapeutic benefit. To reduce possible toxicities, we aimed to maximize local CO levels while limiting systemic exposure of CO. Local delivery of CO-GEMs in diabetic mouse models with either full-thickness wounds or pressure ulcers revealed low systemic levels of CO. The highest average carboxyhemoglobin (COHb), or percentage of hemoglobin bound by CO, was 4.7%, which is well below the 14% that the FDA requires for clinical studies involving CO. The COHb declined over 24 h (Figure S6). There was also no increase in COHb above 4%-5% after daily treatments over the course of 10 days (Figure S7). Baseline levels for untreated mice are between 0% and

#### Figure 2. CO increases cell migration of human dermal fibroblasts in vitro

(A) Percentage of wound closure for in vitro woundhealing assay in dermal fibroblasts exposed to 250 ppm CO for 18 h compared to room air (n = 9). p values were determined by unpaired t test.

(B) Microscopic images showing the migration of human dermal fibroblasts cultured under 250 ppm CO or room air (8× magnification).

2.0%.16 After a single administration of CO-GEM, skin samples were analyzed for CO levels over time (15 min-24 h). The

mean concentration of CO in skin remained above control for up to 24 h (Figure S8). Moreover, there was a significant increase in the concentration of CO in the skin of animals 15 min after the 10<sup>th</sup> daily treatment with CO-GEMs compared to 15 min after the first dose of CO-GEMs (Figure S8).

#### CO-GEMs improved healing of full-thickness wounds in diabetic mice

To study the impact of the CO-GEMs on diabetic wound healing, we developed a system to keep the GEM in place over the wound. We created a molded polyurethane holder to both contain the GEM and keep the wounds clean and was designed to fit the curvature of a mouse body (Figures 4A, 4B, and S9). The holder was adhered to the pre-shaved mouse skin using a tissue adhesive.

Diabetes was induced in C57BL6/J mice by administering streptozotocin once a day for 5 days, at which point blood glucose values were  $\geq$  250 mg/dL (see Table S1). Subsequently, full-thickness wounds were created, and the impact of GEMs on wound healing was evaluated. Full-thickness wounds were generated using a 6 mm dermal biopsy punch, and treatment was initiated after adhering and securing the molded polyurethane holder over the wound. Daily administration of the CO-GEM resulted in significantly reduced wound size compared to N<sub>2</sub>-GEM and untreated controls (Figures 4C, 4D, and S10). Cytokine analysis of tissue lysates demonstrated a reduction in proinflammatory cytokines (interleukin-6 [IL-6], tumor necrosis factor  $\alpha$ , interferon  $\gamma$ ) and an increase in anti-inflammatory cytokines (IL-4 and IL-13) in animals treated with CO-GEM compared to N<sub>2</sub>-GEM and untreated controls (Figures S11 and S12). Next, we evaluated heme oxygenase (HO-1) staining in skin from each treatment group, which revealed that CO-GEM and not N<sub>2</sub>-GEM or untreated controls showed a significant increase in HO-1 expression, suggesting that this cytoprotective gene was involved in wound healing (Figures 4E and 4F).<sup>21</sup> Immunostaining for glutathione (GSH)-protein adducts, a common marker of oxidative stress,22 showed increased protein oxidation in fullthickness wounds of animals treated with N2-GEM or untreated controls, which was significantly suppressed in CO-GEMtreated wounds (Figures 4F-4G).<sup>22</sup>

# CO-GEMs enhanced wound healing of pressure ulcers in diabetic mice

We next tested the impact of CO-GEMs on the healing of pressure ulcers in diabetic mice. The method for creating pressure





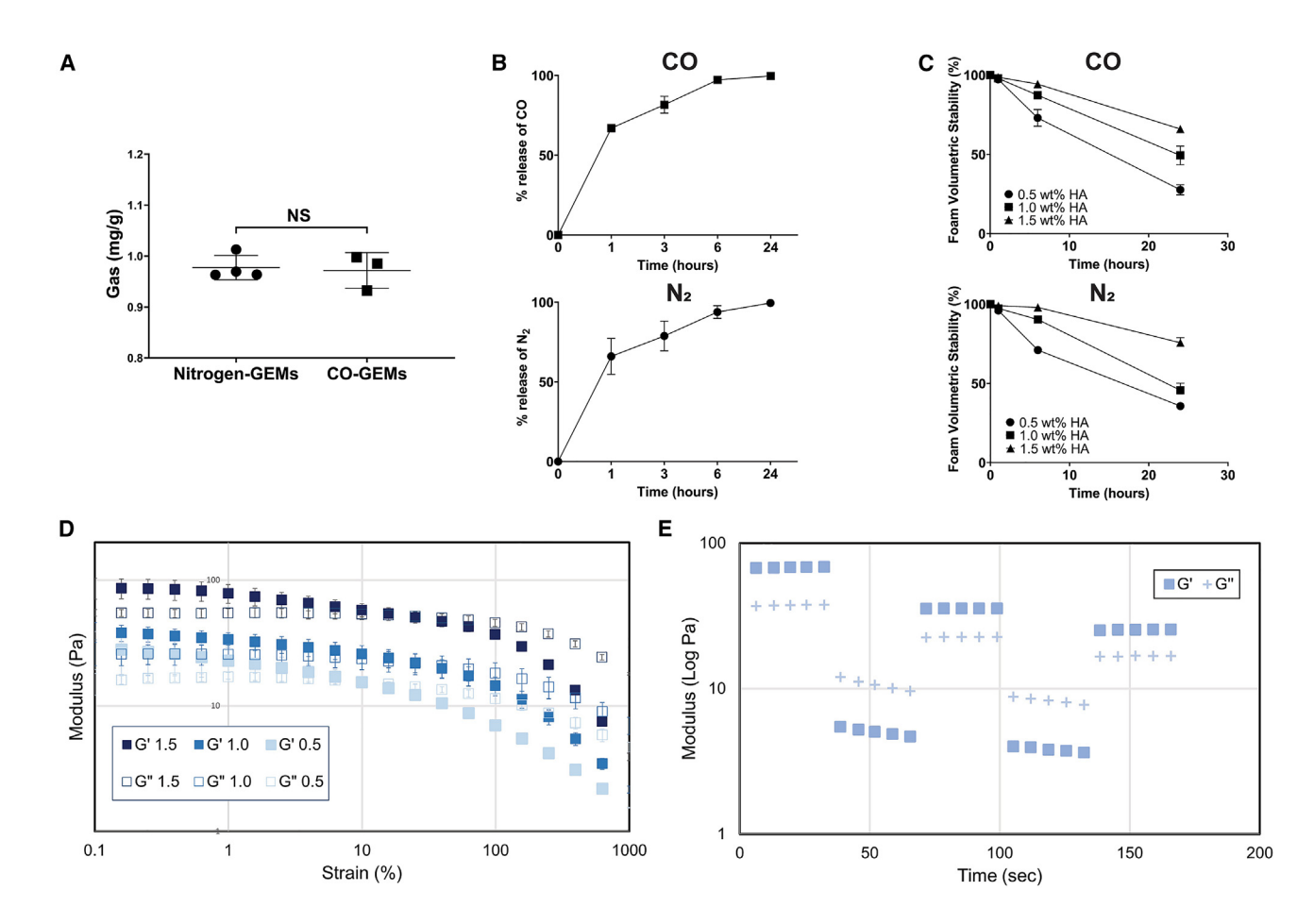


Figure 3. Hyaluronic-acid-based GEMs physically entrap large quantities of gas and exhibit shear-thinning properties

- (A) The concentration of CO and N₂ found in each GEM (n = 3-4 per group). p values were determined by unpaired t test.
- (B) CO and N<sub>2</sub> release kinetics as determined by gas chromatography (n = 4 per group).
- (C) Volumetric foam stability of each GEM based on the type of gas (n = 3 per group).
- (D) Modulus of pressure as a function of the strain, which indicates that all formulations are highly shear thinning (n = 3 per group).
- (E) Modulus of the pressure as a function of step time showing self-healing in foam GEMs with 1.0 wt % hyaluronic acid, which immediately recovered elasticity (G' > G'') at 1% strain after exposure to a high shear strain of 500% (n = 3 per group).

ulcers resulted in two distinct wounds (5 mm apart) on the mouse dorsum. To administer the GEM so that both wounds were covered required a longer holder than what we designed for the full-thickness wound model (Figures 5A, 5B, and S9). All mice received the holder with or without the GEM. Similar to the fullthickness wound model, diabetes was induced by streptozotocin administration, resulting in blood glucose levels ≥250 mg/dL (see Table S1). In the pressure ulcer model, the administration of CO-GEM resulted in significantly decreased wound size compared to the N2-GEM and untreated controls (Figures 5C and 5D). Similar to the full-thickness wound model, histological evaluation revealed increased HO-1 staining in CO-GEM-treated mice compared to N<sub>2</sub>-GEM-treated mice or mice receiving no treatment (Figures 5E and 5F). Staining for GSH showed increased protein oxidation in wounds from animals treated with N<sub>2</sub>-GEM or untreated controls. The expression of oxidative stress markers was significantly suppressed in CO-GEM-treated mice compared to controls (Figures 5F and 5G).

### **DISCUSSION**

The complexity of wound healing is uniquely challenging in patients with diabetes due to chronic inflammation, increased microbial growth associated with increased interstitial glucose levels, and decreased angiogenesis. Several methods have attempted to address one or all of these issues for patients with diabetes using different approaches, as there remains a clear unmet clinical need (Table S2).23-31

Gas therapy administered using GEMs is a unique approach that can enhance wound healing and is amenable to any gas or gas mixture since the gas is entrapped in microbubbles. We studied CO-GEM given its clear benefit across a variety of disorders, including ischemia reperfusion injury, colitis, shock, cancer, and radiation proctitis, among others. 16 Although CO has been shown to modulate endothelial cell proliferation and even migration speed, 18 we found that CO enhanced fibroblast cell migration in vitro in a wound scratch model. These findings then motivated

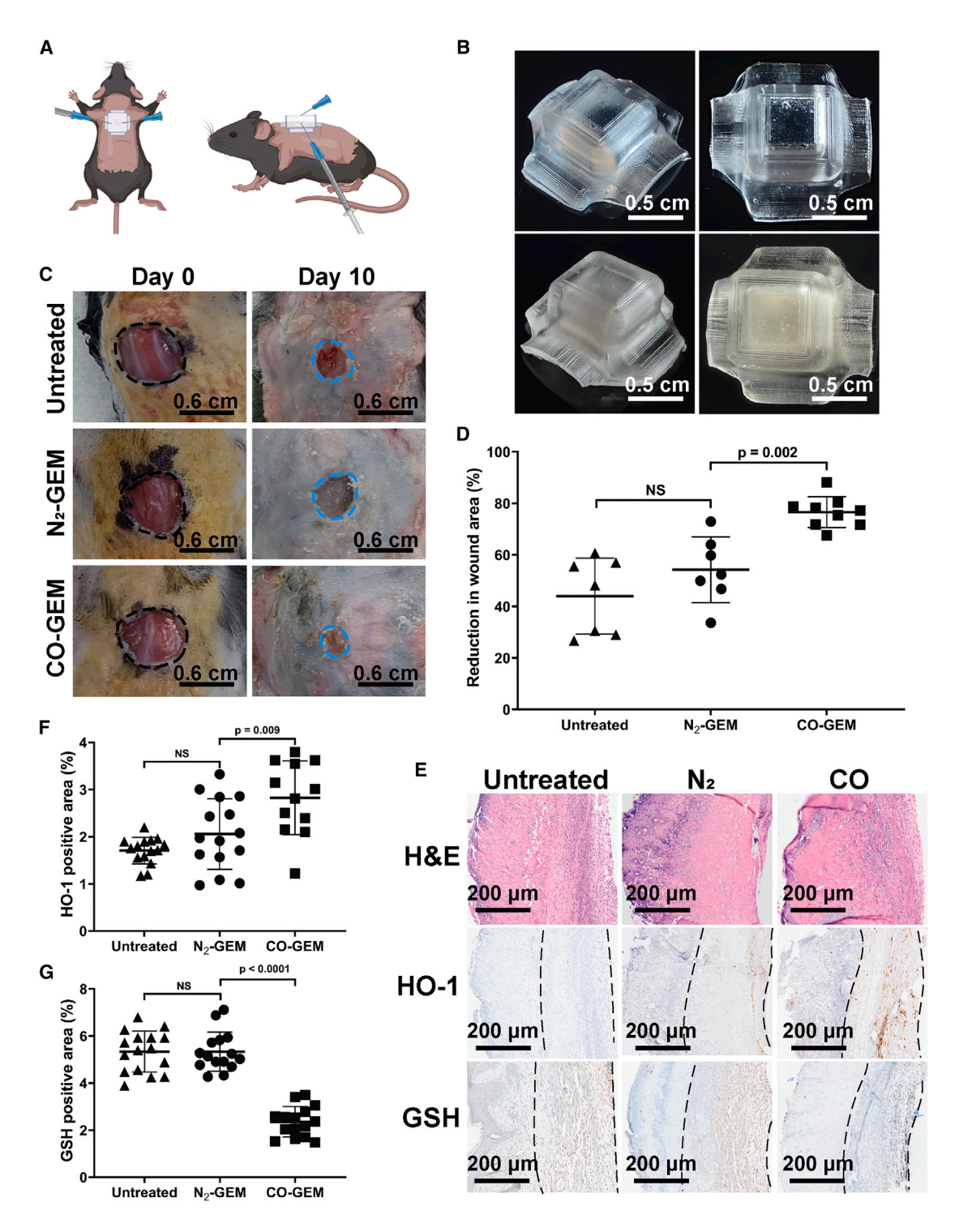


Figure 4. CO-GEMs improved full-thickness wound healing in diabetic mice

- (A) Schematic of the polyurethane GEM holder adhered to the dorsum of a mouse.
- (B) Polyurethane GEM holder adhered to the dorsum of a mouse.
- (C) Representative images of full-thickness wounds at days 0 and 10.
- (D) Reduction in wound area for diabetic mice with full-thickness wounds exposed to CO-GEM or N<sub>2</sub>-GEM or that were untreated (n = 7-9 per arm), demonstrating that CO-GEMs significantly improve wound healing.

(legend continued on next page)





the testing of topical CO in vivo in the form of a CO-GEM. Our tests revealed that topical treatment with a CO-GEM resulted in reduced oxidative stress and improved wound healing in two diabetic wound mouse models with minimal systemic CO exposure.

Other studies have demonstrated the benefit of low-dose CO on skin disorders, including diabetic wound healing, and tendon injury. 14,15,32 HO-1-deficient mice showed delayed wound healing in part due to lack of CO generation. 33 Mechanistically, CO has been shown to inhibit production of pro-inflammatory molecules, to promote the release of anti-inflammatory factors, and to directly modulate free radical generation and secondary oxidative species. 16,34 We observed a significant increase in expression of HO-1 and decreased immunoreactive GSH in the tissue of CO-GEM-treated mice compared to controls. Overexpression of HO-1 by CO may suggest a feedforward mechanism, as has been observed in liver-injury models, 35,36 and may speak to the effects of CO to promote cell migration and/or proliferation. These processes correlated with reduced inflammation and oxidative stress at the site of injury and created a more favorable environment for wound healing to occur. Furthermore, CO has been shown to promote local vasodilation and angiogenesis and reduce oxidative stress, which act synergistically to accelerate and promote an environment conducive to wound healing. 15

The translatability of these findings is fully dependent on the safety of the materials used to topically deliver CO. The materials described here are considered GRAS as defined by the FDA, as well as low cost.37 The materials are found in general wound dressings and cosmetics.<sup>38</sup> Further, all clinical trials of inhaled CO completed to date have concluded that CO treatment is extremely safe, especially in immunocompromised patients such as those who have interstitial pulmonary fibrosis. 39-41 Physician acceptance of CO therapy might be further enhanced if there was a more convenient method for CO delivery, such as the use of CO-GEM.<sup>34</sup> Additionally, a topically delivered agent lends itself to administration outside of a hospital setting, which may reduce cost and barriers to treatment. For broad application, the development of individual pressurized metered dosing systems is essential. Special attention will be given to safety measures to limit toxicity, considering CO is the primary therapy. Moreover, clinical testing against other technologies will be needed to demonstrate a benefit above current systems.

We acknowledge that improvements in the dosing of CO-GEM will require additional formulation testing in healthy subjects, as well as new containment methods for CO-GEMs over wounds. Although topical delivery of CO-GEMs in mice resulted in safe levels of systemic CO exposure, well below the FDA COHb limit of 14%, further testing will need to be done to ensure that this same level can be achieved in humans. Moreover, our study used mouse models of diabetic wound healing, which are often limited because rodent wounds heal primarily by contraction, while humans heal by re-epithelialization.<sup>42</sup> Thus, examining CO-GEMs in animal models that are more reflective of human skin and wounds such as in guinea pigs or pigs would facilitate

translation.43 Another factor to consider is that the diabetic mouse models in our study involved chemically induced pancreatic beta islet cell death and therefore may be less reflective of type 2 diabetic subjects.44 While blood glucose levels are dramatically increased in streptozotocin-induced diabetes, the slow progression of diabetes, including vascular and neural changes, is a slightly different condition to manage. 44 This might be overcome by using animal models with a more prolonged development of diabetes, including insulin-resistant, dietinduced, obese mice. 45 An additional potential confounding issue is that CO may impact the diabetic state and thus have an indirect effect on wound healing. Future studies will examine the impact of CO on blood glucose control in diabetic states.

Taken together, we have developed a topical gas therapy that we call GEMs using FDA GRAS materials otherwise used in clinically available wound-healing products. The topical use of GEMs containing CO resulted in significantly improved wound healing in diabetic mouse models.

#### **EXPERIMENTAL PROCEDURES**

#### Resource availability

#### Lead contact

For additional information and resource requests, please contact Professor James Byrne (james-byrne@uiowa.edu).

#### Materials availability

The study did not produce new unique reagents.

#### Data and code availability

The main article and supplemental information contain all the data presented in the study. Additional information can be requested from the corresponding author.

#### Study design

The aim of this study was to evaluate the topical delivery of CO for diabetic wound management. Safe, low-cost materials were used to topically deliver CO via GEMs. The GEMs were produced using pressurized systems and were tested in vitro and in vivo. First, the in vitro impact of CO on wound healing was determined in cultured fibroblasts, and then the in vivo efficacy of a lead CO-GEM was determined using two different diabetic wound mouse models, full-thickness wounds and pressure ulcers, followed by systemic pharmacodynamic analyses. The Institutional Animal Care and Use Committees at the University of Iowa (2022467-010) approved the use of animals and the proposed protocols. The pathologist was blinded to study arms before and during histological analysis; the investigators and animal technicians were not blinded. All animals were included in the analyses.

# **GEM** formulation development

The GEMs were prepared as described previously. 16,17 In short, a pre-foam solution was prepared by adding 0.8 wt % methylcellulose (Modernist Pantry) and 1.0 wt % high-molecular-weight hyaluronic acid (Bulk Naturals) to 400 mL 1× phosphate-buffered saline (PBS) while heating and stirring the solution. The pre-foam solution was degassed for >8 h prior to use. After degassing, 100 mL pre-foam solution and 0.5 g silver nanopowder (Thermo Scientific) were added to a modified iSi 1-pint whipping siphon with a custom-made M22-1/4 NPT connector to enable pressurization via gas cylinder. This mixture was pressurized to 200 PSI with either CO or N2 (Linde) for 30 s and then shaken for 30 s prior to administration. The CO-enriched PAA solution was prepared similarly to methods from Takagi et al. 14 CO-PAA samples underwent

<sup>(</sup>E) Representative images of immunohistochemical analysis of tissue staining with H&E, HO-1, and GSH at day 10 (4× magnification). The dashed line indicates the wound area analyzed.

<sup>(</sup>F) Quantification of HO-1-positive area (n = 15 images analyzed per arm [3 images per mouse for a total of 5 mice]).

<sup>(</sup>G) Quantification of GSH-positive area (n = 15 images analyzed per arm [3 images per mouse for a total of 5 mice]). p values were determined by one-way ANOVA.

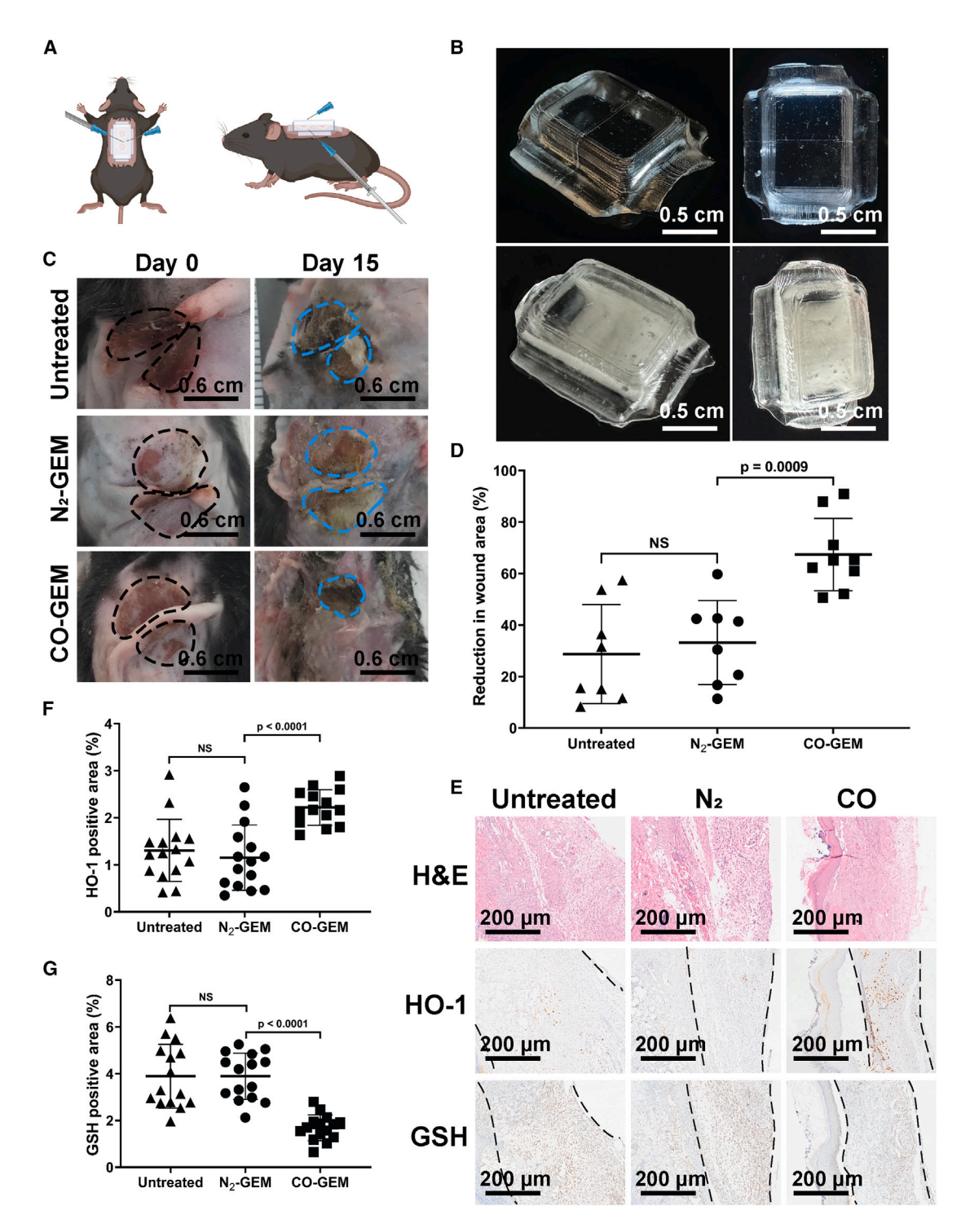


Figure 5. CO-GEMs enhanced wound healing in a pressure ulcer model in diabetic mice

(A) Schematic of the polyurethane GEM holder adhered to the dorsum of a mouse.

(legend continued on next page)

<sup>(</sup>B) Polyurethane GEM holder adhered to the dorsum of mice.

<sup>(</sup>C) Representative images of pressure ulcer wounds at days 0 and 15.

<sup>(</sup>D) Reduction in wound area for diabetic mice with pressure ulcer wounds exposed to CO-GEM or N2-GEM or that were untreated (n = 8-9 per arm), demonstrating CO-GEMs significantly improve wound healing.





three vacuum carbon dioxide (CO2, 99.9%) purge cycles before gas quantification. CO was introduced into a room temperature PAA solution in a closed system, maintained at a low flow rate (~5 PSI), for 15 min, allowing for pressure release. Subsequently, 5 mL of the resulting CO-PAA solution was dispensed into borosilicate glass gas chromatography (GC) vials. To ensure complete CO release, the samples were shaken at 23°C for 72 h. Each sample was then run in quintuplicate on the GC thermal conductivity detector (GC-TCD), with calibration curves generated using the 99.3% CO cylinders that had been used to generate the CO-PAA solution.

#### Material characterization

The GEMs were studied and characterized both macroscopically and microscopically. An EVOS microscope (10× magnification) was used to evaluate the size of the gas bubbles in CO-GEMs over time. The distribution of bubble sizes was determined by placing 1 mL CO-GEM foam into a 24-well plate and performing serial microscopy at designated times. To quantify gases (CO and N<sub>2</sub>) in the GEMs, we used an Agilent GC-TCD with helium as the carrier gas. Before gas quantification, CO-GEM samples underwent three vacuum carbon dioxide (CO<sub>2</sub>, 99.9%) purge cycles. To release CO completely, the samples were subsequently placed into borosilicate glass GC vials and shaken at 37°C for 48 h. Each sample was then run in triplicate on the GC-TCD, with calibration curves generated using the 99.3% CO cylinders that had been used to generate the CO-GEM. For release kinetic analysis of the N2-GEM samples and to reduce background N2 contamination for N2-GEM analysis, the samples were placed in a PLAS-LABS 855-AC Controlled Atmosphere Chamber filled with CO2. The volumetric stability of the different GEMs was determined by placing 100 mL samples into a 250 mL graduated cylinder, maintaining them in a humidified chamber at 37°C, and recording the foam volume and liquid volume fractions at designated times, based on visual inspection.

#### In vitro studies Scratch assav

Adult human dermal fibroblast cells were harvested and counted to 50,000 cells per 500  $\mu$ L. The inserts were placed into the well, and 250  $\mu$ L of the prepared stock of cells was injected into each side of the wound insert. Cells were allowed to grow around the wound area in an incubator (at 37°C, 5% CO<sub>2</sub>) for 12 h. Following this incubation period, the inserts were carefully removed using sterile tweezers, revealing the wound. To evaluate the impact of 250 ppm CO exposure, the plates were then introduced into a hypoxia chamber and flushed with 250 ppm CO containing 5% CO<sub>2</sub>-balanced air, followed by placement into a 37°C incubator. Control plates were then placed into a standard 5% CO<sub>2</sub> incubator. To evaluate the impact of CO-GEMs, 0.5 mL sterile CO-GEM was placed on the top of cell media and then introduced into a hypoxia chamber, followed by placement into a 37°C incubator. Control plates were administered room air-GEM and then introduced into a hypoxia chamber, followed by placement into a 37°C incubator. Each plate was incubated and imaged at 18 h to observe migration. A  $4\times/0.16$  magnification was used for imaging. and the wounds were measured using a scale bar and ImageJ software.

#### Cell viability assays

Adult human dermal fibroblast cells (Coriell Institute, derived from a 28-year-old male) were seeded on 96-well plates with a density of 6,000 cells per well. Twenty-four hours after seeding, the cells were placed in a closed exposure system (STEMCELL Technologies) containing 5% CO2-balanced air, with or without 250 ppm CO, for a subsequent 48 h. Cell viability was assessed using the alamarBlue assay (Thermo Scientific) following guidelines provided by the manufacturer. The resultant absorbance was captured with a microplate instrument (Bio-Rad Laboratories) employing a 560/590 nm (excitation/emission) filter setting. Each experimental condition was replicated three times. The resulting data were adjusted in relation to the untreated sample, which was benchmarked at 100% cell viability. For prolonged cell viability evaluation, 400 human dermal fibroblast cells were seeded into each well of 96-well plates.

At 24 h post-seeding, an alamarBlue assay was performed on 5 wells for each plate, and this was considered day 0. Subsequently, plates were separated for daily CO treatment or normal incubator conditions. The CO-exposed plate was placed in a hypoxia chamber and flushed with 250 ppm CO for 1 h per day. The room air plate was maintained in normal incubator conditions. Five wells from each plate was read daily, and then the cells continued with daily treatments. Immunohistochemistry staining and analysis

Sections of 4% paraformaldehyde-fixed paraffin-embedded tissue samples, cut at  $5-\mu m$  thickness, were used for H&E, GSH, and HO-1 immunostaining. Slides were deparaffinized and stained in an automated staining system (Discovery Ultra, Roche) using tyramide-based developing reagents (Roche/ Ventana Medical Systems), cover slipped, and digitized on a VS200 slide scanner (Olympus). For H&E staining, hematoxylin and eosin (Thermo Scientific) were used. For GSH staining, rabbit polyclonal anti-GSH (Abcam, ab9443) primary was used and followed by OmniMap anti-rabbit (Roche) secondary. For HO-1 staining, rabbit monoclonal anti-HO1 (Abcam, 52947) primary was used and followed by goat anti-rabbit (Vector Laboratories, BA-1000) secondary.

#### **Animal studies**

Male C57BL6/J mice (Jackson Laboratories) aged 6 weeks were allowed to acclimate to the facility for 3 days. To induce diabetes, 50 mg/kg streptozotocin (Sigma-Aldrich) was dissolved in a 4.5-pH citrate buffer before being administered via intraperitoneal injection under brief manual restraint. The 50 mg/kg dose was administered each day for 5 days. 46 On day 6 (day after last dose of streptozotocin), blood from a tail vein nick was obtained and analyzed for blood glucose levels. Mice with blood glucose levels >250 mg/ dL were considered diabetic and were used in the study.

#### Development of polyurethane holders to retain GEMs on animals

A flexible holder was designed and created to retain the GEMs in place on the mice above the wound (Figures 4B and 5B). Two different holder sizes were designed to accommodate the difference in size for the full-thickness wounds versus the pressure ulcers. SolidWorks 2023 was used to design the mold for the GEM holder. The mold was 3D printed using a Form2 printer using durable resin. A 1:1 mixture of ClearFlex 30 Part A and Part B (Smooth-On) was degassed and poured into the cavity of the mold. After a 24-h curing period, the holders were demolded, trimmed, and autoclaved for subsequent application on animal subjects.

#### **Efficacy studies**

Full-thickness wound model. Hair was removed from the mouse dorsum with a chemical depilatory 1 day before wound creation. To create the wound, the mouse was first anesthetized. Then, a 6-mm dermal biopsy punch was traced onto the mouse dorsum, and the site was sterilized with an alcohol wipe followed by a betadine solution. Next, forceps were used to lift the skin, and surgical shears were used to cut the circular wound. The wound was then measured length (L) × width (W) with a caliper, a photo was taken of the initial wound, and the GEM holder was secured to the surrounding skin using a veterinary adhesive. To administer the GEM, the mouse was anesthetized, and a 26-gauge needle was placed in the side of the holder to alleviate pressure. Then 300  $\mu L$  of GEM was administered through a syringe and a separate 26G needle into the holder, directly on top of the wounded area. The needles were removed at the same time. The administration of GEMs was repeated once a day for 10 days. On day 11, the holder was removed, and the wound was measured using calipers and photographed. The wounds were analyzed using ImageJ software (v.1.54d, Java 1.8.0\_345). To ensure accurate measurements, scaling was performed on each individual photo by referencing a ruler positioned to the left of the wounded area. The oval tool within ImageJ was employed to measure the wounded area, and the size of the oval was confirmed with the caliper measurements. Researchers responsible for these measurements were blinded to the treatment groups.

Blood was collected via cardiac puncture. For tissue analysis, a section of the skin (2 × 2 cm) was collected and placed in formalin followed by 70%

<sup>(</sup>E) Representative images of immunohistochemical analysis of tissue stained with H&E, HO-1, and GSH at day 15 (4× magnification). The dashed line indicates the wound area analyzed.

<sup>(</sup>F) Quantification of HO-1-positive area (n = 15 images analyzed per arm [3 images per mouse for a total of 5 mice]).

<sup>(</sup>G) Quantification of GSH-positive area (n = 15 images analyzed per arm [3 images per mouse for a total of 5 mice]). p values were determined by one-way ANOVA.

**Device** 



ethanol and then mounted in paraffin and sectioned for H&E, HO-1, and GSH immunohistochemistry staining. ImageJ software was used to quantify each type of staining in 15 different tissue sections.

Pressure ulcer model. Hair was removed from the mouse dorsum with a chemical depilatory 1 day before pressure ulcer creation. To create the pressure ulcer, the mouse was first anesthetized. Using an established method, 47 two 5-mm magnets were placed 5 mm apart on the mouse dorsum, pinching a fold of the mouse's skin together for 12 h, and then were removed. After 12 h, the magnets were reapplied. This was repeated once more for a total of three cycles, yielding two pressure ulcers separated by  $\sim\!\!1$  mm of normal skin. The ulcers were measured (L × W) with a caliper, a photo was taken of the initial ulcers, and the holder was secured to the surrounding skin using a veterinary adhesive. To administer the GEM, the mouse was anesthetized, and a 26G needle was placed in the side of the holder to alleviate pressure. Then,  $600 \, \mu L$  GEM was administered through a syringe and a separate 26G needle into the holder, directly on top of the wounded area. The needles were removed at the same time. The administration of GEMs was repeated once a day for 10 days. On day 15, the holder was removed, and the wound was measured using calipers and photographed. Blood was collected via cardiac puncture. For tissue analysis, a section of the skin (2 × 2 cm) was collected and placed in formalin followed by 70% ethanol and then mounted in paraffin and sectioned for H&E, HO-1, and GSH immunohistochemistry staining. ImageJ software was used to quantify each type of staining in 15 different tissue sections.

Tissue analysis of CO. Hair was removed from the mouse dorsum with a chemical depilatory, and then the flexible holder was affixed to the dorsum of the mouse using veterinary adhesive. The next day, mice were anesthetized, and a 26G needle was placed in the side of the holder to alleviate pressure. Then, 300  $\mu L$  GEM was administered through a syringe and a separate 26G needle into the holder, directly on top of the wounded area. The needles were removed at the same time. In a subset of mice, the administration of the CO-GEM was delivered once, and then animals were humanely euthanized and skin was sampled over time after treatment (15 min-24 h). In a separate subset of mice, the CO-GEM was administered once a day for 10 days, and then they were humanely euthanized and skin was collected 15 min after the last treatment.

Skin was briefly rinsed with ice-cold PBS to remove any excess blood, and then flash frozen in tubes containing stainless-steel beads and pre-weighed water. For tissue CO analysis, an established method was used<sup>16,48</sup> where tubes were thawed and placed on a bead mill homogenizer for 1 min at maximum speed, followed by 5 min in an ultrasonic bath at room temperature. Tubes were subsequently placed on ice for 15 min. Sealed 2-mL glass, amber borosilicate vials containing 20  $\mu\text{L}$  sulfosalicylic acid (20%) were purged of CO via a custom catalytic converter. Samples were vortexed briefly, and 10  $\mu$ L supernatant was collected in a repeating gas-tight syringe prior to pipetting into the purged amber vials through a rubber septum. The vials were briefly mixed and allowed to sit on ice for 15 min. Using a custom double-needle assembly, the vials were connected to a GC system containing a reducing compound photometer to flush the headspace of the vial through the instrument for CO analysis. The instrument was calibrated daily using a custom gas with a known CO concentration (0.983 ppm CO).

Pharmacodynamic analysis of CO. The pharmacodynamics of CO administered topically using CO-GEM was evaluated in mice. In full-thickness wound mice, conscious mice were treated with 300  $\mu L$  CO-GEM administered into the GEM holder. At designated time points, terminal cardiac punctures were performed, and blood was collected into 1-mL BD syringes filled with 100 units of heparin and analyzed using a RadiometerABL80 FLEX CO-OX blood gas analyzer.

Cytokine analysis. Cytokine analysis was used to evaluate cytokine release in wound tissue lysates. Data analysis was conducted using Python pandas, numpy, scipy, and stats modules. Data were filtered to only include cytokines in which two values above the background rate were present for a given cytokine, indicating a potentially true positive signal. The corrected mean was calculated by subtracting the background value from the mean intensity. The total brightness parameter was calculated by multiplying the corrected mean by the area in which the signal was detected.

Visualizations were created using boxplots and swarmplots, providing both an overview of the data distribution and individual data points. The data were further grouped by "cytokine" and "treatment" and filtered to include only those subsets exhibiting a Z score >0 to account for the cytokines with the highest expression. Data subsets showing a positive standard deviation from the mean were deemed as true positives, indicating a potentially strong response to the gas treatments.

#### Statistical analyses

The data are presented as means ± SD. Graphs were generated using GraphPad Prism software. SAS v.9.3 was used to conduct all analyses. ANOVA was employed to compare continuous values between three or more groups. The random effect was the individual animal ID, to account for individual variability and repeated measures. For cytokine analysis, statistical analyses were performed on the refined data, with a focus on the corrected mean parameter. Since potentially multiple hypotheses were being tested, the Benjamini-Hochberg procedure was utilized to control for false discovery rate. Additionally, to understand the magnitude and significance of any observed differences, effect sizes were calculated using Cliff's Delta. A significance level of p < 0.05 was considered significant.

#### SUPPLEMENTAL INFORMATION

Supplemental information can be found online at https://doi.org/10.1016/j. device.2024.100320.

#### **ACKNOWLEDGMENTS**

We thank the team at SayoStudio for their illustration in Figure 1. The authors also thank the staff of the University of Iowa Central Microscopy Research Facility and Orthopedic Histopathology Service Center for their rapid and detailed work on the histology reported in this study. This work was funded in part by grants from the University of Iowa Hospitals and Clinics Department of Radiation Oncology and the Holden Comprehensive Cancer Center at The University of Iowa and its National Institutes of Health (NIH) National Cancer Institute (NCI) awards P30CA086862 (J.D.B.), NCI K08CA276908 (J.D.B.), American Cancer Society IRG-21-141-46 (J.D.B.), Hope Funds for Cancer Research fellowship (J.D.B.), Prostate Cancer Foundation Young Investigator Award (J.D.B.), Department of Defense Prostate Cancer Program Early Investigator Award (J.D.B.), Department of Defense W81XWH-16-0464 (L.E.O.), National Football League Players Association (L.E.O.), National Science Foundation 1927616 (M.S.T.), Karl van Tassel (1925) Career Development Professorship (G.T.), and the Massachusetts Institute of Technology Department of Mechanical Engineering (G.T.).

#### **AUTHOR CONTRIBUTIONS**

L.E.O. and J.D.B. developed the concept. G.T., L.E.O., and J.D.B. developed the materials and devices. E.W., A.J.L., J.B., M.K.M., A.B.C., S.H., A.T.C., S.U., B.P., A.C.R., A.N.C., J.K., V.F., A.S., and M.C.C. developed the pre-clinical methods and performed the bench and animal studies. M.C.C., M.R.B., D.E.B., M.S.T., G.T., L.E.O., and J.D.B. provided guidance on these experiments. E.W., J.B., S.H., S.U., I.N., M.J., M.C.C., and D.E.B. performed all data analyses. E.W., S.U., and J.D.B. created figures. G.T., L.E.O., and J.D.B. supervised the project. E.W., A.J.L., S.H., S.U., I.N., J.K., M.J., D.E.B., and J.D.B. wrote the paper. All authors discussed the results and edited the manuscript.

#### **DECLARATION OF INTERESTS**

L.E.O. is a scientific advisor to Hillhurst Biopharmaceuticals. J.D.B., L.E.O., and G.T. are co-inventors on a patent application (WO2022055991A1) submitted by Brigham and Women's Hospital, MIT, and BIDMC that covers therapeutic carbon monoxide formulations. Complete details of all relationships for profit and not for profit for G.T. can be found at www.dropbox.com/sh/ szi7vnr4a2ajb56/AABs5N5i0q9AfT1IqIJAE-T5a?dl=0.





Received: November 29, 2023 Revised: January 27, 2024 Accepted: February 14, 2024 Published: March 12, 2024

#### REFERENCES

- 1. American Diabetes Association (2018). Economic Costs of Diabetes in the U.S. in 2017. Diabetes Care 41, 917-928. https://doi.org/10.2337/ dci18-0007.
- 2. Burgess, J.L., Wyant, W.A., Abdo Abujamra, B., Kirsner, R.S., and Jozic, I. (2021). Diabetic Wound-Healing Science. Medicina (Kaunas) 57, 1072. https://doi.org/10.3390/medicina57101072.
- 3. Zubair, M., and Ahmad, J. (2019). Role of growth factors and cytokines in diabetic foot ulcer healing: A detailed review. Rev. Endocr. Metab. Disord. 20, 207-217. https://doi.org/10.1007/s11154-019-09492-1.
- 4. Elraiyah, T., Domecq, J.P., Prutsky, G., Tsapas, A., Nabhan, M., Frykberg, R.G., Hasan, R., Firwana, B., Prokop, L.J., and Murad, M.H. (2016). A systematic review and meta-analysis of debridement methods for chronic diabetic foot ulcers. J. Vasc. Surg. 63, 37S-45S.e2, e31-e32. https://doi. ora/10.1016/i.ivs.2015.10.002.
- 5. Nguyen, T.T., Jones, J.I., Wolter, W.R., Pérez, R.L., Schroeder, V.A., Champion, M.M., Hesek, D., Lee, M., Suckow, M.A., Mobashery, S., and Chang, M. (2020). Hyperbaric oxygen therapy accelerates wound healing in diabetic mice by decreasing active matrix metalloproteinase-9. Wound Repair Regen. 28, 194-201. https://doi.org/10.1111/wrr.12782.
- 6. Anguiano-Hernandez, Y.M., Contreras-Mendez, L., de Los Angeles Hernandez-Cueto, M., Muand Oz-Medina, J.E., Santillan-Verde, M.A., Barbosa-Cabrera, R.E., Delgado-Quintana, C.A., Trejo-Rosas, S., Santacruz-Tinoco, C.E., Gonzalez-Ibarra, J., and Gonzalez-Bonilla, C.R. (2019). Modification of HIF-1alpha, NF-akappaB, IGFBP-3, VEGF and adiponectin in diabetic foot ulcers treated with hyperbaric oxygen. Undersea Hyperb. Med. 46, 35-44.
- 7. Andrews, K.L., Houdek, M.T., and Kiemele, L.J. (2015). Wound management of chronic diabetic foot ulcers: from the basics to regenerative medicine. Prosthet. Orthot. Int. 39, 29-39. https://doi.org/10.1177/03093646 14534296.
- 8. Dasari, N., Jiang, A., Skochdopole, A., Chung, J., Reece, E.M., Vorstenbosch, J., and Winocour, S. (2021). Updates in Diabetic Wound Healing, Inflammation, and Scarring. Semin. Plast. Surg. 35, 153-158. https://doi. org/10.1055/s-0041-1731460.
- 9. Jodheea-Jutton, A., Hindocha, S., and Bhaw-Luximon, A. (2022). Health economics of diabetic foot ulcer and recent trends to accelerate treatment. Foot 52, 101909. https://doi.org/10.1016/j.foot.2022.101909.
- 10. Guan, Y., Niu, H., Liu, Z., Dang, Y., Shen, J., Zayed, M., Ma, L., and Guan, J. (2021). Sustained oxygenation accelerates diabetic wound healing by promoting epithelialization and angiogenesis and decreasing inflammation. Sci. Adv. 7, eabj0153. https://doi.org/10.1126/sciadv.abj0153.
- 11. Chen, C.Y., Wu, R.W., Hsu, M.C., Hsieh, C.J., and Chou, M.C. (2017). Adjunctive Hyperbaric Oxygen Therapy for Healing of Chronic Diabetic Foot Ulcers: A Randomized Controlled Trial. J. Wound Ostomy Continence Nurs. 44, 536-545. https://doi.org/10.1097/WON.000000000000374.
- 12. Hayes, P.D., Alzuhir, N., Curran, G., and Loftus, I.M. (2017). Topical oxygen therapy promotes the healing of chronic diabetic foot ulcers: a pilot study. J. Wound Care 26, 652-660. https://doi.org/10.12968/jowc.2017. 26.11.652.
- 13. Malone-Povolny, M.J., Maloney, S.E., and Schoenfisch, M.H. (2019). Nitric Oxide Therapy for Diabetic Wound Healing. Adv. Healthc. Mater. 8, e1801210. https://doi.org/10.1002/adhm.201801210.
- 14. Takagi, T., Okayama, T., Asai, J., Mizushima, K., Hirai, Y., Uchiyama, K., Ishikawa, T., Naito, Y., and Itoh, Y. (2022). Topical application of sustained released-carbon monoxide promotes cutaneous wound healing in diabetic mice. Biochem. Pharmacol. 199, 115016. https://doi.org/10.1016/j.bcp. 2022.115016.

- 15. Ahanger, A.A., Prawez, S., Kumar, D., Prasad, R., Amarpal, Tandan, S.K., Tandan, S.K., and Kumar, D. (2011). Wound healing activity of carbon monoxide liberated from CO-releasing molecule (CO-RM). Naunvn-Schmiedeberg's Arch. Pharmacol. 384, 93-102. https://doi.org/10.1007/ s00210-011-0653-7.
- 16. Byrne, J.D., Gallo, D., Boyce, H., Becker, S.L., Kezar, K.M., Cotoia, A.T., Feig, V.R., Lopes, A., Csizmadia, E., Longhi, M.S., et al. (2022). Delivery of therapeutic carbon monoxide by gas-entrapping materials. Sci. Transl. Med. 14, eabl4135. https://doi.org/10.1126/scitranslmed.abl4135.
- 17. Bi, J., Witt, E., Voltarelli, V.A., Feig, V.R., Venkatachalam, V., Boyce, H., McGovern, M., Gutierrez, W.R., Rytlewski, J.D., Bowman, K.R., et al. (2023). Low-Cost, High-Pressure-Synthesized Oxygen-Entrapping Materials to Improve Treatment of Solid Tumors. Adv. Sci. 10, e2205995. https://doi.org/10.1002/advs.202205995.
- 18. Wegiel, B., Gallo, D.J., Raman, K.G., Karlsson, J.M., Ozanich, B., Chin, B.Y., Tzeng, E., Ahmad, S., Ahmed, A., Baty, C.J., and Otterbein, L.E. (2010). Nitric oxide-dependent bone marrow progenitor mobilization by carbon monoxide enhances endothelial repair after vascular injury. Circulation 121, 537-548. https://doi.org/10.1161/CIRCULATIONAHA.109. 887695
- 19. Lee, M., Han, S.H., Choi, W.J., Chung, K.H., and Lee, J.W. (2016). Hyaluronic acid dressing (Healoderm) in the treatment of diabetic foot ulcer: A prospective, randomized, placebo-controlled, single-center study, Wound Repair Regen. 24, 581-588. https://doi.org/10.1111/wrr.12428.
- 20. Kalantari, K., Mostafavi, E., Afifi, A.M., Izadiyan, Z., Jahangirian, H., Rafiee-Moghaddam, R., and Webster, T.J. (2020). Wound dressings functionalized with silver nanoparticles: promises and pitfalls. Nanoscale 12, 2268-2291. https://doi.org/10.1039/c9nr08234d.
- 21. Lin, C.C., Hsiao, L.D., Cho, R.L., and Yang, C.M. (2019). Carbon Monoxide Releasing Molecule-2-Upregulated ROS-Dependent Heme Oxygenase-1 Axis Suppresses Lipopolysaccharide-Induced Airway Inflammation. Int. J. Mol. Sci. 20, 3157. https://doi.org/10.3390/ijms20133157.
- 22. Coleman, M.C., Goetz, J.E., Brouillette, M.J., Seol, D., Willey, M.C., Petersen, E.B., Anderson, H.D., Hendrickson, N.R., Compton, J., Khorsand, B., et al. (2018). Targeting mitochondrial responses to intra-articular fracture to prevent posttraumatic osteoarthritis. Sci. Transl. Med. 10, eaan5372. https://doi.org/10.1126/scitranslmed.aan5372.
- 23. Armstrong, D.G., and Lavery, L.A.; Diabetic Foot Study Consortium (2005). Negative pressure wound therapy after partial diabetic foot amputation: a multicentre, randomised controlled trial. Lancet 366, 1704-1710. https:// doi.org/10.1016/S0140-6736(05)67695-7.
- 24. Blume, P.A., Walters, J., Payne, W., Ayala, J., and Lantis, J. (2008). Comparison of negative pressure wound therapy using vacuum-assisted closure with advanced moist wound therapy in the treatment of diabetic foot ulcers: a multicenter randomized controlled trial. Diabetes Care 31. 631-636. https://doi.org/10.2337/dc07-2196.
- 25. Marston, W.A., Hanft, J., Norwood, P., and Pollak, R.; Dermagraft Diabetic Foot Ulcer Study Group. Dermagraft Diabetic Foot Ulcer Study, G (2003). The efficacy and safety of Dermagraft in improving the healing of chronic diabetic foot ulcers: results of a prospective randomized trial. Diabetes Care 26, 1701-1705. https://doi.org/10.2337/diacare.26.6.1701.
- 26. Veves, A., Falanga, V., Armstrong, D.G., and Sabolinski, M.L.; Apligraf Diabetic Foot Ulcer Study (2001). Graftskin, a human skin equivalent, is effective in the management of noninfected neuropathic diabetic foot ulcers: a prospective randomized multicenter clinical trial. Diabetes Care 24. 290-295. https://doi.org/10.2337/diacare.24.2.290.
- 27. Kirsner, R.S., Warriner, R., Michela, M., Stasik, L., and Freeman, K. (2010). Advanced biological therapies for diabetic foot ulcers. Arch. Dermatol. 146, 857-862. https://doi.org/10.1001/archdermatol.2010.164.
- 28. Wieman, T.J., Smiell, J.M., and Su, Y. (1998). Efficacy and safety of a topical gel formulation of recombinant human platelet-derived growth factor-BB (becaplermin) in patients with chronic neuropathic diabetic ulcers. A phase III randomized placebo-controlled double-blind study. Diabetes Care 21, 822-827. https://doi.org/10.2337/diacare.21.5.822.





- 29. Margolis, D.J., Gupta, J., Hoffstad, O., Papdopoulos, M., Glick, H.A., Thom, S.R., and Mitra, N. (2013). Lack of effectiveness of hyperbaric oxygen therapy for the treatment of diabetic foot ulcer and the prevention of amputation: a cohort study. Diabetes Care 36, 1961-1966. https://doi. org/10.2337/dc12-2160.
- 30. Frykberg, R.G., Franks, P.J., Edmonds, M., Brantley, J.N., Téot, L., Wild, T., Garoufalis, M.G., Lee, A.M., Thompson, J.A., Reach, G., et al. (2020). A Multinational, Multicenter, Randomized, Double-Blinded, Placebo-Controlled Trial to Evaluate the Efficacy of Cyclical Topical Wound Oxygen (TWO2) Therapy in the Treatment of Chronic Diabetic Foot Ulcers: The TWO2 Study. Diabetes Care 43, 616-624. https://doi.org/10.2337/dc19-0476.
- 31. Snyder, R., Galiano, R., Mayer, P., Rogers, L.C., and Alvarez, O.; Sanuwave Trial Investigators (2018). Diabetic foot ulcer treatment with focused shockwave therapy: two multicentre, prospective, controlled, doubleblinded, randomised phase III clinical trials. J. Wound Care 27, 822-836. https://doi.org/10.12968/jowc.2018.27.12.822.
- 32. Ruopp, M., Reiländer, S., Haas, D., Caruana, I., Kronenberg, D., Schmehl, W., Stange, R., and Meinel, L. (2023). Transdermal carbon monoxide delivery. J. Control. Release 357, 299-308. https://doi.org/10.1016/j.jconrel 2023 03 034
- 33. Deshane, J., Chen, S., Caballero, S., Grochot-Przeczek, A., Was, H., Li Calzi, S., Lach, R., Hock, T.D., Chen, B., Hill-Kapturczak, N., et al. (2007). Stromal cell-derived factor 1 promotes angiogenesis via a heme oxygenase 1-dependent mechanism. J. Exp. Med. 204, 605-618. https://doi. org/10.1084/jem.20061609.
- 34. Motterlini, R., and Otterbein, L.E. (2010). The therapeutic potential of carbon monoxide. Nat. Rev. Drug Discov. 9, 728-743. https://doi.org/10.
- 35. Kuramitsu, K., Gallo, D., Yoon, M., Chin, B.Y., Csizmadia, E., Hanto, D.W., and Otterbein, L.E. (2011). Carbon monoxide enhances early liver regeneration in mice after hepatectomy. Hepatology 53, 2016-2026. https://doi. org/10.1002/hep.24317.
- 36. Zuckerbraun, B.S., Billiar, T.R., Otterbein, S.L., Kim, P.K.M., Liu, F., Choi, A.M.K., Bach, F.H., and Otterbein, L.E. (2003). Carbon monoxide protects against liver failure through nitric oxide-induced heme oxygenase 1. J. Exp. Med. 198, 1707-1716. https://doi.org/10.1084/jem.20031003.
- 37. Administration, F.a.D. (2023). GRAS Substances (SCOGS) Database.
- 38. Yasin, A., Ren, Y., Li, J., Sheng, Y., Cao, C., and Zhang, K. (2022). Advances in Hyaluronic Acid for Biomedical Applications. Front. Bioeng. Biotechnol. 10, 910290. https://doi.org/10.3389/fbioe.2022.910290.
- 39. Fredenburgh, L.E., Perrella, M.A., Barragan-Bradford, D., Hess, D.R., Peters, E., Welty-Wolf, K.E., Kraft, B.D., Harris, R.S., Maurer, R., Nakahira, K.,

- et al. (2018). A phase I trial of low-dose inhaled carbon monoxide in sepsisinduced ARDS. JCI Insight 3, e124039. https://doi.org/10.1172/jci.insight.
- 40. Rosas, I.O., Goldberg, H.J., Collard, H.R., El-Chemaly, S., Flaherty, K., Hunninghake, G.M., Lasky, J.A., Lederer, D.J., Machado, R., Martinez, F.J., et al. (2018). A Phase II Clinical Trial of Low-Dose Inhaled Carbon Monoxide in Idiopathic Pulmonary Fibrosis. Chest 153, 94-104. https:// doi.org/10.1016/j.chest.2017.09.052.
- 41. Bathoorn, E., Slebos, D.J., Postma, D.S., Koeter, G.H., van Oosterhout, A.J.M., van der Toorn, M., Boezen, H.M., and Kerstjens, H.A.M. (2007). Anti-inflammatory effects of inhaled carbon monoxide in patients with COPD: a pilot study. Eur. Respir. J. 30, 1131-1137. https://doi.org/10. 1183/09031936.00163206.
- 42. Chen, L., Mirza, R., Kwon, Y., DiPietro, L.A., and Koh, T.J. (2015). The murine excisional wound model: Contraction revisited. Wound Repair Regen. 23, 874-877. https://doi.org/10.1111/wrr.12338.
- 43. Seaton, M., Hocking, A., and Gibran, N.S. (2015). Porcine models of cutaneous wound healing. ILAR J. 56, 127-138. https://doi.org/10.1093/ilar/ ilv016.
- 44. Marino, F., Salerno, N., Scalise, M., Salerno, L., Torella, A., Molinaro, C., Chiefalo, A., Filardo, A., Siracusa, C., Panuccio, G., et al. (2023). Streptozotocin-Induced Type 1 and 2 Diabetes Mellitus Mouse Models Show Different Functional, Cellular and Molecular Patterns of Diabetic Cardiomyopathy. Int. J. Mol. Sci. 24, 1132. https://doi.org/10.3390/ijms24021132.
- 45. Yin, T.C., Van Vranken, J.G., Srivastava, D., Mittal, A., Buscaglia, P., Moore, A.E., Verdinez, J.A., Graham, A.E., Walsh, S.A., Acevedo, M.A., et al. (2023). Insulin sensitization by small molecules enhancing GLUT4 translocation. Cell Chem. Biol. 30, 933-942.e6. https://doi.org/10.1016/j. chembiol.2023.06.012.
- 46. Chaudhry, Z.Z., Morris, D.L., Moss, D.R., Sims, E.K., Chiong, Y., Kono, T., and Evans-Molina, C. (2013). Streptozotocin is equally diabetogenic whether administered to fed or fasted mice. Lab. Anim. 47, 257-265. https://doi.org/10.1177/0023677213489548.
- 47. Stadler, I., Zhang, R.Y., Oskoui, P., Whittaker, M.S., and Lanzafame, R.J. (2004). Development of a simple, noninvasive, clinically relevant model of pressure ulcers in the mouse. J. Invest. Surg. 17, 221-227. https://doi.org/ 10.1080/08941930490472046.
- 48. Vreman, H.J., Wong, R.J., Kadotani, T., and Stevenson, D.K. (2005). Determination of carbon monoxide (CO) in rodent tissue: effect of heme administration and environmental CO exposure. Anal. Biochem. 341, 280-289. https://doi.org/10.1016/j.ab.2005.03.019.